We are IntechOpen, the world's leading publisher of Open Access books Built by scientists, for scientists

6,900
Open access books available

186,000
International authors and editors

200M
Downloads

Our authors are among the

154
Countries delivered to

TOP 1%
most cited scientists

12.2%
Contributors from top 500 universities

WEB OF SCIENCE™

Selection of our books indexed in the Book Citation Index in Web of Science™ Core Collection (BKCI)

Interested in publishing with us?
Contact book.department@intechopen.com

Numbers displayed above are based on latest data collected.
For more information visit www.intechopen.com

Chapter 7

Catalytic Activation of PVP-Stabilized Gold/Silver Cluster on p-Nitrophenol Reduction: A DFT

Madhulata Shukla and Indrajit Sinha

Additional information is available at the end of the chapter

http://dx.doi.org/10.5772/intechopen.72097

Abstract

Systematic DFT calculations on poly(N-vinyl-2-pyrrolidone) (PVP) stabilization of Ag13 cluster have shown that the former acts not only as a stabilizer but also plays an important role in activating the Ag catalyst by supplying extra electrons to it through its oxygen atoms. Natural Bonding Orbital (NBO) calculations show that weak back donation of electrons from M(dπ) orbital of Ag to antibonding σ* of one of the N-O bond, facilitates the formation of the nitroso intermediate. Vibrational frequency calculation of PNP association with Ag13-2PVP cluster carried out to understand the extent and the nature of this interaction better. Red shift in the frequencies is result of strong interaction with that of silver cluster present in Ag13-2PVP-PNP model.

Keywords: nanoparticles, p-nitrophenol, DFT calculation, charge distribution, NBO calculation

1. Introduction

Recently nanoparticle (NP) research is an area of adoring scientific research due to wide variety of potential application in different fields of physics, chemistry, material science, medicine and biology, as a result of their unique electronic, optical, magnetic, mechanical, physical, chemical and catalytic properties. Nanoparticle is a microscopic particle with at least one dimension less than 100 nm. The intrinsic properties of metal nanoparticles are mainly determined by their size, shape, composition, stability, crystallinity, structure, etc. The properties of many conventional materials change when formed from nanoparticles. This is typically because nanoparticles have a greater surface area per weight than larger particles which causes them to be more reactive to some other molecules. It can be silver, gold, iron, iron oxide, platinum, silica, titanium oxide, etc. Nanoparticles are of great scientific interest as they

IntechOpen

© 2018 The Author(s). Licensee IntechOpen. This chapter is distributed under the terms of the Creative Commons Attribution License (http://creativecommons.org/licenses/by/3.0), which permits unrestricted use, distribution, and reproduction in any medium, provided the original work is properly cited. CC BY

are effectively a bridge between bulk materials and atomic or molecular structures. Synthesis of M-NPs can proceed by chemical reduction, thermolysis, photochemical decomposition, electro reduction, microwave and sonochemical irradiation. In recent literature there are large number of reports on synthesis, properties and applications of noble metals Au, Ag and Cu NPs [1–3]. This is mainly because all three elements show good localized surface plasmon resonance (LSPR) absorbance in the visible range and also have large number of catalytic applications. However, the high cost of Au and to a lesser extent Ag restrict their applications in many cases. As an alternative of Au and Ag NPs, researchers have investigated Cu nanoparticles. CuNPs are less expensive and exhibit comparably higher electrical conductivity and catalytic activity [4, 5]. The LSPR absorbance of CuNPs in the visible range is comparatively less intense. Another issue is that Cu nanoparticles are easily oxidized [6], yet nanoparticles of copper oxides also have wide applicability as catalysts. Silver NP found to be quite stable and hence chosen for studying the effect of nanostructures on their catalytic activity. In liquid phase nanoparticle synthesis, polymeric molecules are often used for stabilizing nanoparticles against aggregation. The function of the polymers are to avoid the aggregation of the NP in solution and to control the size and shape at the crystallographic level [7–9]. Among various polymeric molecules investigated in literature, polyvinyl pyrrolidone (PVP) has been one of the most frequently used stabilizers since it is non-toxic and soluble in many polar solvents. While such PVP stabilized noble metal nanoparticles have extensively been used as catalysts for various reactions [10, 11], few workers have concentrated in literature on the effect of such stabilizer molecule on the nanoparticle surface on their catalytic properties [12–14]. Nevertheless, only a few research papers have investigated the effect of such stabilization of nanoparticle surfaces on the electronic properties of such nanocomposites. Tsunoyama et al. proposed that electron transfer occurs from the anionic Au cores of Au:PVP into the LUMO (π^*) of O_2 which generates superoxo or peroxo like species. Latter plays a key role in the oxidation of alcohol [10]. Similar mechanisms were proposed by some other related experimental studies as well that the adsorption of PVP on to the catalyst surface can also modify the electronic structure of nanoparticles by charge transfer [15, 16]. Yet several aspects remain unclear, such as whether PVP attaches to the metal surface through its O atom or through the N atom [15, 17]. The strength of interaction of PVP with the metal surface is also another aspect that needs to be investigated. Finally, the most important question that in a catalytic reaction how does the interaction between the catalyst surface and the reactant/substrate change in presence of stabilizer. Very few reports are available regarding this topic [18, 19]. The catalytic reduction of nitroarenes to aminoarenes by transfer hydrogenation methodologies is an important class of organic transformations. The reaction does not occur even in the presence of strong reductants like metal hydrides unless catalyzed by a suitable nanocatalyst [12]. Synthesis of silver NP using PVP has been reported in our earlier study [20]. PVP stabilized Ag nanoparticles have often been successfully used as catalysts for such reactions [14, 20]. However, to the best of our knowledge, there is no detailed DFT study on effect of PVP (poly(N-vinyl-2-pyrrolidone)) stabilization of Ag cluster on its catalytic activity with respect to a nitroarene (p-nitrophenol) substrate. In this chapter, we first carry out DFT calculations on Ag/Au cluster along with the monomer of PVP moiety using Gaussian program. Further, the effect of PVP stabilized Ag clusters (catalyst) on p-nitrophenol (PNP) has been investigated in detail. Energy of interaction found by the B3LYP level of calculation elucidates

the stability of the moieties. Mechanism for activation of the nitro group and formation of nitroso intermediate has been proposed from NBO analysis. IR study of the Ag cluster stabilized by PVP and its effect on PNP has been studied in detail using DFT calculation.

2. Computational procedure

A 13 atom silver and gold cluster is carved out of the FCC Ag/Au lattice constructed using the MAPS software (Scienomics). The Gaussian 03 program [21] package employed for the DFT calculations at the Becke's three parameter functional and Lee–Yang–Parr hybrid functional (B3LYP) level [22, 23] of calculation. LaNL2DZ for Ag/Au and 6-31G++(d,p) basis set for C, H, N and O atoms was used while performing DFT calculation. B3LYP functional calculations give the stable cluster and also reproduce the experimental results [17, 18, 24]. Calculations are carried out for ground state geometry optimization in gaseous phase. The Mulliken charges of each atom are calculated by the Mulliken population analysis. NBO analysis and IR frequency calculation performed to find out the strength of interaction of nitro group of PNP with silver cluster.

3. Results and discussion

3.1. Geometry optimization and Mulliken charge distribution

Au13 and Ag13 cluster (magic number) were optimized using B3LYP method and LaNL2DZ basis set using Gaussian program [25, 26]. Optimized structure of Ag13 and Au13 has been shown in **Figure 1(a)** and **(b)** respectively. Mulliken charge present on each atom is shown clearly. Several literature are available explaining the charge distribution on gold and silver cluster by varying number of atoms attached as well as by varying the shape of the clusters [24, 25]. It has been reported by Chen and Johnston [25] that charges on atoms vary with variation in shape of

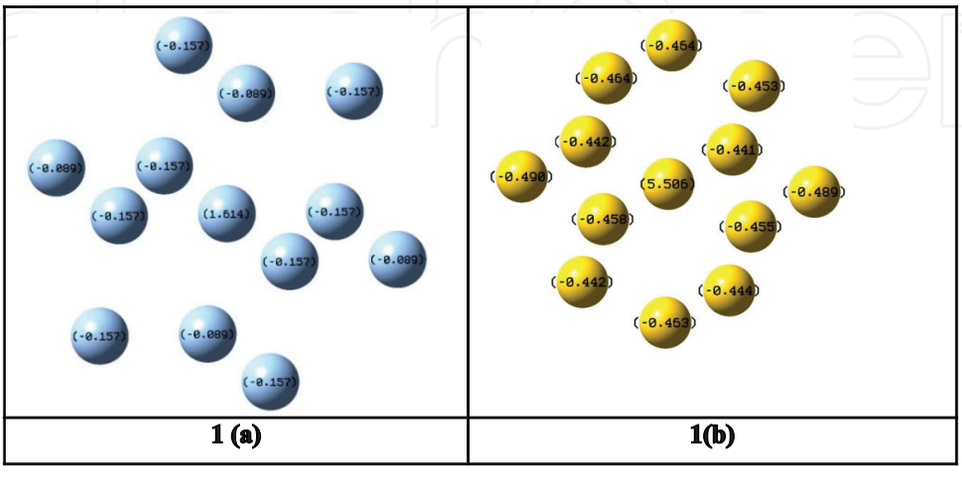

Figure 1. Optimized structure of (a) Ag13 cluster and (b) Au13 cluster with their Mulliken charges present on it.

the cluster. Mulliken charges present in the pure Ag13 Ih (icosahedral) cluster are +0.256 for the central Ag atom and −0.022 for a peripheral Ag atom. The charges in the pure Au13 Oh (cuboctahedral) cluster are +0.379 for the central Au atom and −0.033 for a peripheral Au atom. Hence, the structural order in 13-atom icosahedral (Ih) and cuboctahedral (Oh) clusters also induces charge transfer from the central atom to the peripheral ones. Varying the number of atoms in an alloy changes the property of nanoparticles drastically. It has been shown that with introduction of single Au/Ag atom in Ag13/Au13 cluster, charge present on each atom vary hugely. Stability of nanoalloys comes from a directional charge transfer induced by the structural order, which is added to that induced by the electronegativity difference between unlike atoms. As the Pauling electronegativity of Au (2.4) is greater than that of Ag (1.9), there is a degree of charge transfer from Ag to Au atoms [25]. It is clear from **Figure 1(a)** and **(b)** that charge present on gold is quite higher than that of silver atom. Central atom has huge positive charge as compared to negative charge on the surface. Also one can say that gold is more active catalyst as compared to silver. Okumura et al. [24] had presented the DFT calculation of gold nanoparticle stabilized with PVP at B3LYP level of calculation. Role of PVP on the catalytic activities of gold cluster has been explained very well and in refined way. Presence of PVP not only acts as a stabilizer to prevent aggregation, but also activates the catalyst by supplying charge to it. Calculations have shown that the charge transfer from the adsorbed PVP to Au13 produces negatively charged O_2 on Au13-4PVP. Hence one can conclude that the catalytic activities of Au clusters are affected by the adsorbed PVPs. Varying the number of adsorbed PVP, charge present on the catalyst vary drastically. Similar observation was observed for the silver cluster (Ag13) in our calculation. This is the first report explaining the effect of PVP on the silver cluster.

Optimized structure of Ag13-2PVP with the charge present on each atoms are clearly has been shown in **Figure 2**. Distance between oxygen of PVP and different silver atoms are 2.32 and 2.36 Å. It clearly shows that interaction of PVP with silver cluster is quite strong. Also charge present on bare Ag13 cluster and Ag13 surrounded by 2 PVP moieties are quite different. Higher charge on the surface silver atom of Ag13-2PVP is indicative of the fact that PVP does not just acts as a stabilizer, but activates the catalyst as well, similar as obtained by Okumura et al. for gold cluster [24].

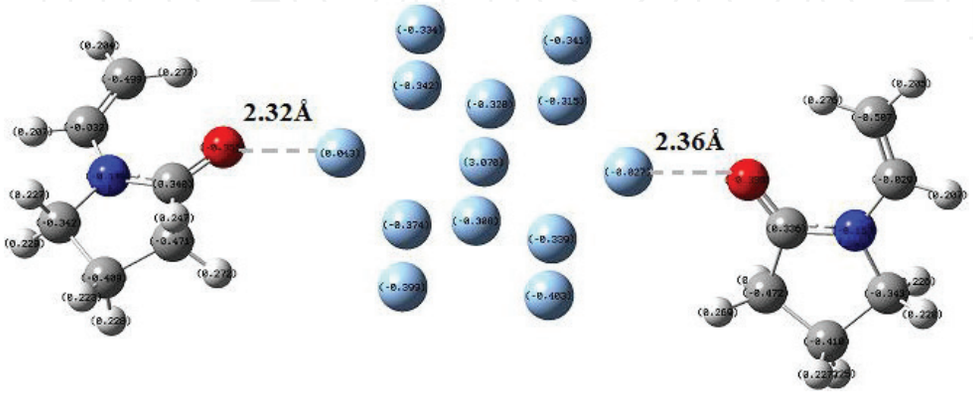

Figure 2. Optimized structure of Ag13-2PVP moiety with charge present on each atom.

3.2. Effect of p-nitrophenol on silver cluster surrounded by PVP

Among the available nitroarenes, the reduction of p-nitrophenol (PNP) using NaBH4 as the reductant has been studied extensively as a model pollutant and catalytic reduction reaction [27]. Several literatures are available for this catalytic reduction reaction. In recent study, it has been investigated that during catalytic reduction of p-nitrophenol to p-aminophenol (AP) glycerol as the reductant also in a mixture of glycerol and water as the reaction medium [20]. Several experimental literatures are available for this reduction reaction [27] but the actual mechanism for this catalytic reduction of p-nitrophenol to p-aminophenol is still unclear. Hence to study the catalytic reduction mechanism DFT proves to be very useful [28].

To study the catalytic reduction mechanism, p-nitrophenol was incorporated in the optimized structure of Ag13-2PVP moiety and reoptimized the whole system at same B3LYP level of calculation. Optimized structure of PNP and Ag13-2PVP-PNP has been shown in **Figure 3(a)** and **(b)** respectively. Important geometrical parameters such as bond length, bond angles have been shown in **Table 1**. It has been observed that N-O bond length increases from 1.28 Å (in PNP) to 1.36 Å in Ag13-2-PVP-PNP moiety. N11-C1 bond length decreases by 0.05 Å when PNP interact with Ag13 cluster. <O12-N11-O13 decrease by ~3° when interact with Ag13 cluster. Ag7----C24=O25, Ag4----C41=O42 distance found to be 2.32 and 2.36 Å. This shows strong interaction with silver cluster and PVP molecules. Ag1-O60 and Ag2-O59 bond length calculated to be 2.28 and 2.27 Å, which clearly shows that PNP is much closer and interacting strongly with silver cluster than that of PVP molecule.

3.3. Electronic effect due to PVP interaction with nanoparticle

Figure 4(a) and **(b)** shows the Mulliken charge distribution of Ag13 and Ag13-2PVP moiety (shown by different colors). Negative charge on Ag13 is symmetrically distributed among the shell Ag atoms of the cluster. This is balanced by the electropositive central Ag atom (shown by green color). Charges on shell silver atoms of the Ag cluster (before interaction) found to be either −0.09 or −0.15. Charge on central silver atom is detected to be +1.61. This result is similar with that as reported by Li and Chen [29] and Chen and Johnston [25]. To balance the negative

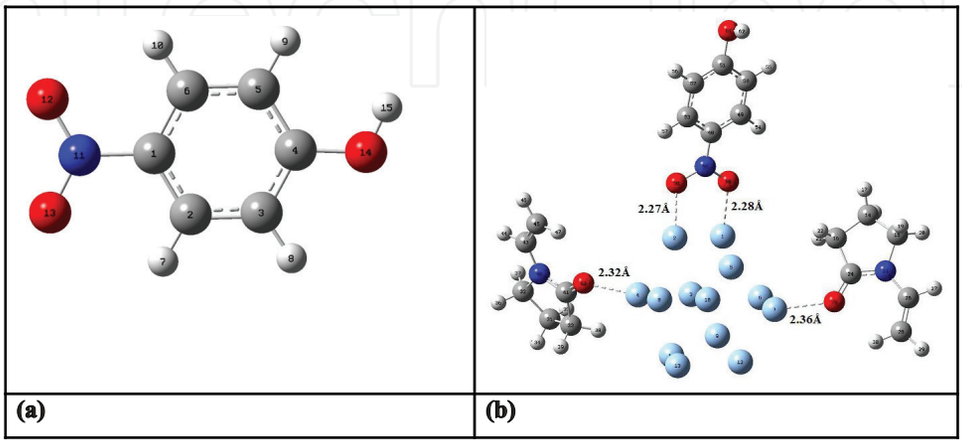

Figure 3. Optimized structure of (a) p-nitrophenol and (b) Ag13-2-PVP-PNP moiety.

Parameters [bond length (Å)/bond angles (°)]	Data obtained from DFT calculation
p-nitrophenol (PNP)	
N11-O12	1.28
N11-C1	1.46
<O12-N11-O13	123.51
<O12-N11-C1	118.23
Ag13-2-PVP-PNP	
N58-O59	1.36
N58-C48	1.41
Ag1-O60	2.28
Ag2-O59	2.27
<O59-N58-O60	120.83
<O59-N58-C48	119.71
Ag7----C24=O25	2.32
Ag4----C41=O42	2.36

Table 1. Selected bond length, bond angles of different system obtained from DFT calculation.

charge present on shell atoms, core becomes positively charged to neutralize and stabilized the whole cluster. As PVP interacts with the Ag13 cluster, charge distribution becomes asymmetrical. The charges present on shell Ag atoms interacting with (PVP) O atoms are −0.07 and −0.05. Rest of the shell Ag atoms have charges more or less around −0.30. The central Ag atom is most electron deficient carrying charge of +3.07. Adsorption of the PVP model molecule onto the surface of Ag13 increases the negative charge density on Ag13 cluster, similar as for Au13 cluster explained by Okumura et al. [24]. With adsorption of PVP on the surface, catalyst becomes more active due to increase of negative charge on the Ag13 surface. To reduce the computational cost, PVP has been removed for further interaction study of PNP with Ag13. Optimized structure of PNP and Ag13-PNP has been shown in **Figure 4(c)** and **(d)** along with their respective charges. Variation in charges on different atoms of PNP before and after interaction has been clearly shown by the different colored atoms of **Figure 4(e)** and **(f)** respectively.

These interactions of PNP with that of Ag13 are better understood from electrostatic potential (ESP) charge distribution shown in **Figure 5**. Orange color represents the negative electron density around the electronegative oxygen atoms.

3.4. Natural bonding orbital (NBO) analysis

Stabilization energy E(2) found to be proportional to the charge transfer energy or charge distribution energy [30]. For each donor NBO(i) and acceptor NBO(j), the stabilization energy E(2) associated with delocalization of electron pair from donor orbital (i) to acceptor orbital (j) and is defined as

http://dx.doi.org/10.5772/intechopen.72097

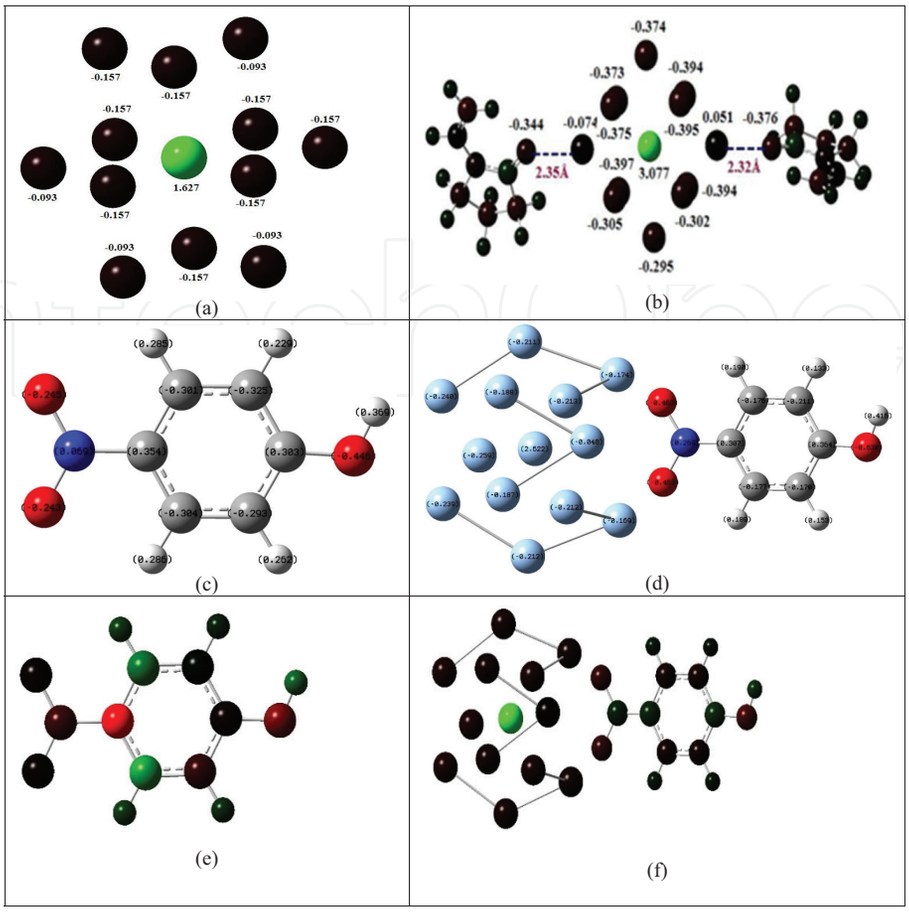

Figure 4. Mulliken charge distribution on different atoms of (a) Ag13 cluster and (b) Ag13-2PVP (c) PNP (d) Ag-PNP. Colour representation of Mulliken charge on different atoms of (e) PNP (f) Ag13-PNP. Red colour represents the most electronegative and green colour represents the most electropositive atom.

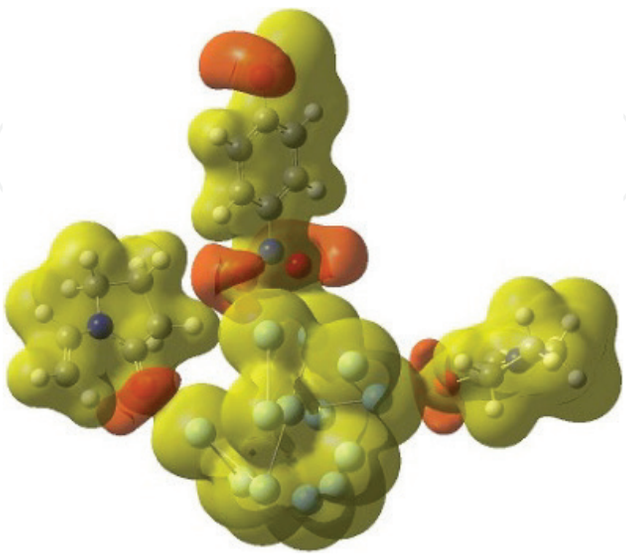

Figure 5. Electrostatic potential charge distribution on Ag13-2PVP-PNP moiety.

$$E(2) = \Delta E_{ij} = \frac{q_i F(i,j)^2}{\varepsilon_i - \varepsilon_j} \quad (1)$$

where q_i is the donor orbital occupancy, ε_i and ε_j are the diagonal elements (orbital energies). F(i, j) is the interaction element between donor and acceptor orbitals and is known as diagonal NBO Fock matrix element. The delocalization effects can be identified by means of off-diagonal elements of the Fock matrix. The forces of these delocalization interaction, E(2) (kcal/mol), are estimated by second order perturbation theory [31]. E(2) term corresponding to these interactions can also be the total charge transfer energy in the molecule.

To better understand the interaction between Ag13 cluster and PNP molecules, NBO calculation carried out at same B3LYP level of calculation. **Table 2** presents the major interaction present between silver cluster and PNP through both the oxygen atoms of the latter. It has been observed from **Table 2** that in addition to charge transfer from the oxygen (of the nitro group) to Ag atom, there is also a back donation of electron from M(dπ) orbital of Ag2 to antibonding σ* of N58-O59 [E(2) = 2.06 kcal/mol]. Further, the back donation of electron from M(dπ) orbital of Ag1 to antibonding σ* of N58-O60 is comparatively much weaker [E(2) = 0.71 kcal/mol]. This shows that only one of the two N-O bonds is considerably weakened by this back donation of electron from Ag atoms in comparison to the other N-O bond. Hence, from these obtained NBO results, one can predict the subsequent formation of nitroso compound as an intermediate. This mechanism is in agreement with the one proposed by Liu et al. in an experimental study for reduction of nitrobenzene in presence of Ag catalyst [12] and for reduction of PNP in presence of Ag catalyst by Gu et al. [27].

3.5. Calculated vibrational spectra and analysis of calculated IR spectra of PNP and Ag13-2PVP-PNP

IR frequency calculations prove to be a good tool for predicting the interaction present in a molecule [31]. For better analysis of the interaction of PNP with silver cluster, we perform the

Donor orbital (i)	Acceptor orbital (j)	Second order perturbation stabilization energy E(2)/(kcal/mol)
149. LP*(6)Ag2	564. BD*(1)N58-O59	2.06
262. LP(1)O60	142. LP*(8)Ag1	1.97
264. LP(3)O60	140. LP*(6)Ag1	5.21
264. LP(3)O60	141. LP*(7)Ag1	4.68
264. LP(3)O60	142. LP*(8)Ag1	1.39
261. LP(3)O59	149. LP*(6)Ag2	6.45
261. LP(3)O59	150. LP*(7)Ag2	3.17
260. LP(2)O59	150. LP*(7)Ag2	2.04
259. LP(1)O59	150. LP*(7)Ag2	4.02
55. BD(1)N58-O60	150. LP*(7)Ag2	0.71

Table 2. Significant donor-acceptor NBO interactions in Ag cluster and PNP moiety with calculated second order stabilization energies E(2) (kcal/mol).

IR frequency calculations on the optimized structure of Ag13-2PVP-PNP moiety at same B3LYP level of calculation and same basis set as mention above. To analyze the changes that occurred in the vibrational spectrum due to such association we contrast it with the calculated IR frequencies of the optimized structure of PNP alone. Calculated data has been presented in **Table 3**. For the same vibrational motion, the frequency of the peak present in PNP varies significantly when it is associated with the silver cluster. Scissoring of O-N-O occurs at 621 cm^{-1} in PNP while it is observed at 588 cm^{-1} (red shift of 33 cm^{-1}) when there is interaction with Ag cluster. Similarly, a strong red shift of 131 cm^{-1} is observed when PNP interacts with silver cluster for benzene ring breathing coupled with C-O(H) stretching and O-N-O scissoring motion in PNP. It is due to coupling of NO_2 with that of the silver cluster. Another strong red shift of 103 cm^{-1} is observed for

Wavenumber/(cm^{-1})/ Ag13-2PVP-PNP	Intensity	Wavenumber (cm^{-1})/PNP	Intensity	Difference in wavenumber/(cm^{-1})/ [Ag13-2PVP-PNP-(PNP)]	Assignment of bands
588	85	621	27	33	O-N-O scissoring in PNP
710	65	841	30	131	Benzene ring breathing coupled with C-O(H) stretching and O-N-O scissoring in PNP
864	58	887	68	23	Out of plane bending of C-H in PNP
1113	85	1124	118	11	C-H in plane bending coupled with O-N-O asymmetric stretching in PNP
1167	356	1170	246	3	C-O-H scissoring in PNP coupled with C-H in plane bending
1174	41	1277	341	103	O-N-O symmetric stretching in PNP
1192	32	1204	81	12	H-C=C-H scissoring in PNP
1267	53	1287	55	20	C-O(H) stretching in PNP
1322	42	1277	341	45	C-N stretching in PNP
1520	190	1529	32	9	C-H in plane bending in PNP coupled with C-N stretching
1645	60	1657	120	12	C=C stretching in PNP
3185	34	3210	10	25	C-H asymmetric stretching in PNP coupled with C-O-H scissoring
3708	91	3704	81	4	O-H stretching in PNP

Table 3. DFT calculated IR frequency of NB and Ag13-2PVP-PNP at B3LYP level.

O-N-O symmetric stretching in PNP. For other vibrational motions, difference in wavenumbers has been shown in **Table 3**. Red shifts in most of the frequencies are due to strong interaction of PNP with silver cluster present in Ag13-2PVP-PNP model. Hence IR frequency calculation proves to be a good tool in predicting the strength of interaction present in a molecule [32].

4. Conclusions

DFT calculations on PVP stabilized Ag13 cluster have shown that the PVP acts not only as a stabilizer but also plays an important role in activating the Ag catalyst by supplying extra charge to it, mainly through oxygen atom. Electrostatic potential (ESP) charge distribution demonstrates that nitro group in p-nitrophenol (PNP) interacts strongly through oxygen end with the Ag cluster. Furthermore, Natural Bonding Orbital (NBO) analysis shows that there is weak back donation of electron from M(dπ) orbital of Ag to antibonding σ^* of one of the N-O bonds while the other N-O bond in PNP is not affected. Therefore, one of the N-O bonds is drastically weakened in comparison to other N-O bond. Hence the formation of the nitroso intermediate will assist its further reduction reaction. Hence stabilization energy calculation can be a good tool in predicting the intermediate in a reaction catalyzed by NPs, which is difficult to predict experimentally. Finally, significant red shifts in calculated IR frequencies are a consequence of strong interaction of PNP with silver cluster present in Ag13-2PVP-PNP model. Hence, IR frequency calculation is a good tool for predicting the strength of interaction present in a molecule.

Acknowledgements

Computer Centre, BHU and Computer Unit, IIT-BHU is acknowledged for providing the computational facility. SERB (PDF/2017/002589) is acknowledged for providing financial support.

Author details

Madhulata Shukla[1,2]* and Indrajit Sinha[1]

*Address all correspondence to: madhu1.shukla@gmail.com

1 Department of Chemistry, Indian Institute of Technology (Banaras Hindu University), Varanasi, India

2 G.B. College, Ramgarh, Kaimur, Veer Kunwar Singh University, Kaimur, India

References

[1] Iravani S, Korbekandi H, Mirmohammadi SV, Zolfaghari B. Synthesis of silver nanoparticles: chemical, physical and biological methods. Research in Pharmaceutical Sciences. 2014;**9**:385-406

[2] Stamplecoskie KG, Scaiano J. Optimal size of silver nanoparticles for surface-enhanced Raman spectroscopy. Journal of Physical Chemistry C. 2011;**115**:1403-1409

[3] Duan XC, Ma JM, Lian JB, Zheng WJ. The art of using ionic liquids in the synthesis of inorganic nanomaterials. CrystEngComm. 2014;**16**:2550-2559

[4] Choi CS, Jo YH, Kim MG, Lee HM. Control of chemical kinetics for sub-10 nm Cu nanoparticles to fabricate highly conductive ink below 150 °C. Nanotechnology. 2012;**23**:065601 8pp

[5] Wu T, Huang Q, Li W, Chen G, Ma X, Zeng G. Electroreduction of copper dichloride powder to copper nanoparticles in an ionic liquid. Journal of Nanomaterials. 2014;**399**:6. Article ID 751424

[6] Muzikansky A, Nanikashvili P, Grinblat J, Zitoun D. Ag dewetting in Cu@Ag monodisperse core–shell nanoparticles. Journal of Physical Chemistry C. 2013;**117**: 3093-3100

[7] Bratlie KM, Lee H, Komvopoulos K, Yang P, Somorjai GA. Platinum nanoparticle shape effects on benzene hydrogenation selectivity. Nano Letters. 2007;**7**:3097-3101

[8] Zhang GH, Guo WL, Wang XK. Sonochemical formation of nanocrystalline gold in aqueous solution. Materials Research Innovations. 2007;**11**:201-206

[9] Tao AR, Habas S, Yang P. Shape control of colloidal metal nanocrystals. Small. 2008;**4**: 310-325

[10] Tsunoyama H, Ichikuni N, Sakurai H, Tsukuda T. Effect of electronic structures of Au clusters stabilized by poly(N-vinyl-2-pyrrolidone) on aerobic oxidation catalysis. Journal of the American Chemical Society. 2009;**131**:7086-7093

[11] Quintanilla A, Butselaar-Orthlieb VCL, Kwakernaak C, Sloof WG, Kreutzer MT, Kapteijn F. Weakly bound capping agents on gold nanoparticles in catalysis: Surface poison? Journal of Catalysis. 2010;**271**:104-114

[12] Liu X, Cheng H, Cui P. Catalysis by silver nanoparticles/porous silicon for the reduction of nitroaromatics in the presence of sodium borohydride. Applied Surface Science. 2014;**292**:695-701

[13] Vadakkekara R, Chakraborty M, Parikh PA. Reduction of aromatic nitro compounds on colloidal hollow silver nanospheres. Colloids and Surfaces A: Physicochemical and Engineering Aspects. 2012;**2014**:11-17

[14] Tejamaya M, Romer I, Merrified RC, Lead JR. Stability of citrate, PVP, and PEG coated silver nanoparticles in ecotoxicology media. Environmental Science & Technology. 2012; **46**:7011-7017

[15] Xian J, Jiang QHZ, Ma Y, Huang W. Size-dependent interaction of the poly(N-vinyl-2-pyrrolidone) capping ligand with Pd nanocrystals. Langmuir. 2012;**28**:6736-6741

[16] Aguilar JG, Garcia MN, Murcia AB, Mori K, Kuwahara Y, Yamashita H, Amoros DC. Evolution of the PVP–Pd surface interaction in nanoparticles through the case study of formic acid decomposition. Langmuir. 2016;**32**:12110-12118

[17] Abdelghany AM, Mekhail MS, Abdelrazek EM, Aboud MM. Combined DFT/FTIR structural studies of monodispersed PVP/gold and silver nano particles. Journal of Alloys and Compounds. 2015;**646**:326-332

[18] Boekfa B, Pahl E, Gaston N, Sakurai H, Limtrakul J, Ehara M. C–Cl bond activation on Au/Pd bimetallic nanocatalysts studied by density functional theory and genetic algorithm calculations. Journal of Physical Chemistry C. 2014;**118**:22188-22196

[19] Nunzi F, Angelis FD, Selloni A. Ab initio simulation of the absorption spectra of photoexcited carriers in TiO_2 nanoparticles. Journal of Physical Chemistry Letters. 2016;**7**:3597-3602

[20] Verma AD, Mandal RK, Sinha I. Glycerol as green hydrogen source for catalytic reduction over anisotropic silver nanoparticles. RSC Advances. 2016;**6**:103471-103477

[21] Frisch MJ, Trucks GW, Schlegel HB, Scuseria GE, Robb MA, Cheeseman JR, Montgomery JA Jr, Vreven T, Kudin KN, Burant JC, Millam JM, Iyengar SS, Tomasi J, Barone V, Mennucci B, Cossi M, Scalmani G, Rega N, Petersson GA, Nakatsuji H, Hada M, Ehara M, Toyota K, Fukuda R, Hasegawa J, Ishida M, Nakajima T, Honda Y, Kitao O, Nakai H, Klene M, Li X, Knox JE, Hratchian HP, Cross JB, Bakken V, Adamo C, Jaramillo J, Gomperts R, Stratmann RE, Yazyev O, Austin AJ, Cammi R, Pomelli C, Ochterski JW, Ayala PY, Morokuma K, Voth GA, Salvador P, Dannenberg JJ, Zakrzewski VG, Dapprich S, Daniels AD, Strain MC, Farkas O, Malick DK, Rabuck AD, Raghavachari K, Foresman JB, Ortiz JV, Cui Q, Baboul AG, Clifford S, Cioslowski J, Stefanov BB, Liu G, Liashenko A, Piskorz P, Komaromi I, Martin RL, Fox DJ, Keith T, Al-Laham MA, Peng CY, Nanayakkara A, Challacombe M, Gill PMW, Johnson B, Chen W, Wong MW, Gonzalez C, Pople JA. Gaussian, Inc. Wallingford, CT. 2004

[22] Lee C, Yang W, Parr RG. Development of the Colle-Salvetti correlation-energy formula into a functional of the electron density. Physical Review B. 1988;**37**:785-789

[23] Becke AD. Density-functional thermochemistry. III. The role of exact exchange. The Journal of Chemical Physics. 1993;**98**:5648-5652

[24] Okumura M, Kitagawa Y, Kawakami T, Haruta M. Theoretical investigation of the hetero-junction effect in PVP-stabilized Au_{13} clusters. The role of PVP in their catalytic activities. Chemical Physics Letters. 2008;**459**:133-136

[25] Chen F, Johnston RL. Charge transfer driven surface segregation of gold atoms in 13-atom Au–Ag nanoalloys and its relevance to their structural, optical and electronic properties. Acta Materialia. 2008;**56**:2374-2380

[26] Shin K, Kim DH, Yeo SC, Lee HM. Structural stability of AgCu bimetallic nanoparticles and their application as a catalyst: A DFT study. Catalysis Today. 2012;**185**:94-98

[27] Gu S, Wunder S, Lu Y, Ballauff M. Kinetic analysis of the catalytic reduction of 4-nitrophenol by metallic nanoparticles. Journal of Physical Chemistry C. 2014;**118**: 18618-18625

[28] Pozun ZD, Rodenbusch SE, Keller E, Tran K, Tang W, Stevenson KJ, Henkelman G. A systematic investigation of *p*-nitrophenol reduction by bimetallic dendrimer encapsulated nanoparticles. Journal of Physical Chemistry C. 2013;**117**:7598-7604

[29] Li W, Chen F. A density functional theory study of structural, electronic, optical and magnetic properties of small Ag–Cu nanoalloys. Journal of Nanoparticle Research. 2013;**15**:1809-1822

[30] Gineityte V. On the relation between the stabilization energy of a molecular system and the respective charge redistribution. Journal of Molecular Structure (THEOCHEM). 2002;**585**:15-25

[31] Reed AE, Curtiss LA, Weinhold F. Intermolecular interactions from a natural bond orbital, donor-acceptor viewpoint. Chemical Reviews. 1988;**88**:899-926

[32] Shukla M, Srivastava N, Saha S. Theoretical and spectroscopic studies of 1-butyl-3-methylimidazolium iodide room temperature ionic liquid: Its differences with chloride and bromide derivatives. Journal of Molecular Structure. 2010;**975**:349-356

IntechOpen

IntechOpen

IntechOpen